The conditions for tidal bore formation and its effect on the transport of saline water at river mouths

Article *in* Water Resources · January 2013

DOI: 10.1134/S0097807813010028

CITATIONS
14

READS
1,191

1 author:

E. N. Dolgopolova
Russian Academy of Sciences
45 PUBLICATIONS **104** CITATIONS

SEE PROFILE

ISSN 0097-8078, Water Resources, 2013, Vol. 40, No. 1, pp. 16–30. © Pleiades Publishing, Ltd., 2013.
Original Russian Text © E.N. Dolgopolova, 2013, published in Vodnye Resursy, 2013, Vol. 40, No. 1, pp. 19–35.

HYDROPHYSICAL PROCESSES

The Conditions for Tidal Bore Formation and Its Effect on the Transport of Saline Water at River Mouths

E. N. Dolgopolova

Water Problems Institute, Russian Academy of Sciences, ul. Gubkina 3, Moscow, 119333 Russia
E-mail: dolgopolova@gmail.com

Received September 15, 2011

Abstract—Approaches to the mathematical description of bore propagation upstream a river in its mouth area are briefly reviewed. Data on some river mouths, where bores were observed, are given, and the conditions of their formation are considered. The existence of a bore is determined by tide magnitude, river runoff, and the depth profile in the estuary. The same factors govern seawater penetration distance into river mouths, the degree of mixing of seawater and river water, and the regularities of sediment motion at river mouths. The types of water circulation at the mouths of the greatest rivers, where bore takes place, are considered, and its effect on seawater intrusion range into river mouths is analyzed. The results of comparison of the effect of channel training on bore existence conditions and the propagation range of saline water into the estuaries of the Seine (France) and Qiantang (China) are given.

Keywords: mouth, tide, bore, sea and river water mixing, saltwater intrusion
DOI: 10.1134/S0097807813010028

INTRODUCTION

Tidal bore is a water surge, propagating upstream during tide water level rise, the main cause of which is large tide amplitude. The tide height can be enhanced by local factors, in particular, by resonance, if the oscillation period of water level in a bay or an estuary is close to the tide period [20]. In that case, a tidal bore can form two days after the maximal tide.

The bore generally forms during spring tide at the largest change of water level. The small depths of flows at river mouths and the funnel-like shape of estuary increase the range of level variations, especially, when river runoff is low. The water entering the funnel-like, shallow river mouth rapidly moves upstream the river as a steep wave with a velocity of up to ~12 m/s. The wave front extends all across the river; it is almost rectilinear, and when not, it is concave upstream the river. When water level rises rapidly, the water depth distribution becomes discontinuous and a hydraulic jump appears. The bore wave forms after low water, and during the upstream propagation of the tidal wave, the frontal part of the wave in narrow and shallow parts of the river becomes very steep, often rising 1–2 m above the low-water level. The bore may disappear in wider and deeper parts of river channel and reappear in narrower and shallower parts further upstream. A foamy crest forms above the frontal part of the wave in shallow river segments. The first wave is commonly followed by several waves with lower heights. After the passage of the bore, water level in some rivers rises, though not reaching the height of the bore wave crest, while in other rivers, the level rise is continuous. As the water level in the given place rises further, the bore stops not long before the high water. The distance covered by the bore wave upstream the river varies in different rivers from a few kilometers to ~70–80 km.

According to estimates of different authors, more than 400 estuaries in all continents, except for Antarctic are known to experience the effect of bores [20, 22, 25]. The formation of the bore depends primarily on tide amplitude, which, in its turn, depends on the geographic position of the river's mouth. It also depends on the shape of the river mouth. Bores take place in the mouth areas of estuarine and estuarine–deltaic types, according to the river mouth classification proposed in [9]. Most authors mention bores that form at the mouths of large rivers, the major of which are the estuaries of the rivers of Seine and Gironde (France), Severn and Mersey (Great Britain), Qiantang (Hangzhou, China), Styx and Daly (Australia), Batang Lupar (Malaysia), Hooghly Branch of the Ganges R. (India), individual branches with estuarine widening in the Amazon R. (Brazil), Cook Inlet (Alaska), and the Bay of Fundy (USA) [37]. Table 1 gives some characteristics of those rivers and bores, arranged in the descending order of their bore wave height.

Researchers disagree in the assessment of the tide range at which bore formation begins; thus, a minimal range of 6 m is given in [13], while in [20], it is noted that bore wave can also form at mouths with lower tide range (4 m).

Table 1. Characteristics of river mouths in which tidal bore forms, arranged in the ascending order of bore wave height h_b: water flow Q; the volume ratio of fresh W to sea water P_t, entering the estuary during the tidal cycle; tidal range h; the rate of estuary width change dB/dl; the upper and lower values of parameters—before and after channel training; dash means no data available or no phenomenon

River or estuary name, country	Q, m^3/s	W/P_t	h, m	h_b, m	dB/dl	Fr_b
Qiantang, China	1000	$\frac{0.01}{0.022}$	8.9	4.0	$\frac{0.23}{\sim 0.1}$	2.5
Branch of the Amazon, Brazil	1.72×10^5	–	6	3.5	–	1.03
Hooghly Branch, India	$1.4–3.5 \times 10^3$	0.04	4.9	1–3	0.18	1.01
Yangtze Northern Branch, China	366.6	0.01	3.3	~1.5	0.16	1.21
Severn, Great Britain	107	0.001	15.0	1.5	0.24	1.04
Gironde: Garonne and Dordogne, France	$\frac{941}{810}$	0.01	6.0	1.5	0.13	$\frac{1.04}{2.3}$
Mersey, Great Britain	56.0	0.001	8.4	<1	0.29	1.01
Seine*, France	430	$\frac{0.024}{0.08}$	7.5	–	$\frac{0.54}{0.38}$	–
Mezen**	780	0.03	7.8	–	0.2	0.5

Notes: * In the Seine, the bore has not appeared since channel training;
** In the Mezen R., no bore is observed, despite the high tide.

In this study, we give the major approaches to the mathematical description of bore wave propagation in a river mouth reach and consider the conditions of its formation. The effect of the ratio of river water flow, tide range, and the shape of the mouth on the formation of bore wave, as well as the effect of this wave on seawater intrusion into the mouth is considered. The results of present-day studies of bore wave propagation into the mouths of some large rivers are given, and the effect of river training activities on the bore formation conditions is considered.

MATHEMATICAL DESCRIPTION OF THE PHENOMENON

Tidal oscillations of ocean surface, which cause variations in water level in the mouth section, produce unsteady currents at river mouths. When water level rises during flood tide, the tidal wave becomes steeper until it forms an abrupt front—a tidal bore. After its formation, an abrupt increase in water depth appears at the front, and the water flow in this case can be described with the help of moving hydraulic jump [38].

A method of description of water wave motion (which often forms as the result of manipulation of hydroengineering dam gates, the functioning of hydropower stations following different control schedules, emergency water releases, water runoff variations due to floods, etc.) was developed in the hydraulics, based on solving a system of two equations: a one-dimensional differential equation of motion (Saint-Venant dynamic equilibrium equation) and a continuity equation for a nonsteady flow in an open channel [14, 15]. At wave motion, water flow Q and the flow cross-section area A are functions of time t and distance x (the x-axis is directed along the estuary). When the tide is high enough, the perturbation section is a source of a wave or a series of waves, which transfer considerable water masses (the so-called, translation waves), unlike wind waves, whose characteristic feature is the oscillatory motion of water particles in the vertical plane relative their initial positions and the low capacity of transferring water mass. When water level abruptly rises during flood tide, a reverse positive wave forms in the perturbation section and propagates upstream the river, causing an increase in A upstream the perturbation section and a decrease in the wave motion velocity U both in time and along its path. The abrupt level drop during ebb tide results in the formation of a reverse negative wave, which transfers a drop in water level in the open channel upstream the river. The reverse positive wave has a steep leading front, while the negative wave has a gentle leading front, which flattens during its motion. The wave water motion at tidal river mouths, including the tidal bore, is generally a sum of the positive and negative reverse waves [14]. Saint-Venant [20] was the first to suggest a mathematical description of the motion of a bore wave in the Seine R.

The motion of bore wave can be regarded as a quasi-steady hydraulic jump, moving upstream with velocity V (Fig. 1). The integral form of mass and momentum conservation equations yields a series of

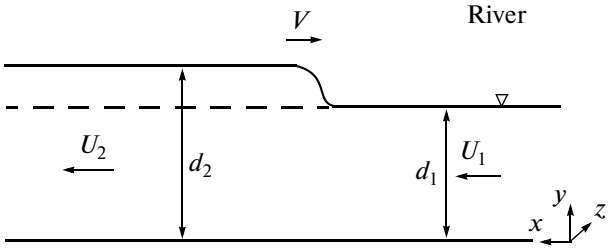

Fig. 1. Scheme of interaction between bore wave and river flow.

relationships describing variations in flow characteristics at the moment of passage of bore front:

$$(U_1 + V)d_1 = (U_2 + V)d_2, \quad (1)$$

$$\frac{1}{2}\rho g(d_2^2 - d_1^2) = \rho(U_1 + V)d_1(\beta_1(U_1 + V) - \beta_2(U_2 + V)), \quad (2)$$

where U is the cross-section-averaged flow velocity, directed positively downstream toward river mouth, d is water depth, g is gravity acceleration, β is Boussinesq momentum coefficient. The subscripts 1 and 2 refer to the initial and the new flow conditions that vary due to the passage of the bore (Fig. 1). Equations (1) and (2) were written under the assumption that the pressure distributions upstream and downstream of the bore front are hydrostatic; friction losses are assumed negligible; the river bed in the short segment where bore forms is assumed horizontal. The solution of equations (1) and (2) yields the dependence of the ratio of conjugate depths (d_1/d_2) on the Froude number (Fr_b) for a tidal bore [15, 20]:

$$\frac{d_1}{d_2} = \frac{1}{2}\left(\sqrt{1 + 8\mathrm{Fr}_b^2} - 1\right), \quad (3)$$

$$\text{where } \mathrm{Fr}_b = \frac{U_1 + V}{\sqrt{gd_1}}. \quad (4)$$

In the case of a bore, we always have $\mathrm{Fr}_b > 1$ and the expression $(\mathrm{Fr}_b - 1)$ is a measure of bore size. When $\mathrm{Fr}_b < 1$, the tidal wave cannot become a bore.

The results of measurements of flow characteristics during bore passage in a natural estuary and in laboratory flumes confirm the abrupt changes in velocity and pressure fields, typical of hydraulic jump [20]. An experimental study of d_2/d_1 in flume bore simulation has shown this ratio to generally satisfy the continuity and momentum conservation equations [38]. However, in the range $1.1 < \mathrm{Fr}_b < 2$, the measurements of d_2/d_1 ratio give an underestimation with respect to (3) because of the involvement of air in the wave crest of the collapsing bore.

Two types of tidal bores are known: undular and breaking; the undular tidal bore takes place at $1 < \mathrm{Fr}_b < 1.8$, while at $\mathrm{Fr}_b > 1.8$, the bore becomes a breaking one. In practice, the majority of bores has a wavy shape: the first wave is followed by a chain of well-developed wavy formations with smaller amplitude. The oscillations of the free surface of a wavy bore can be described mathematically with the help of well-known equations of wave transformation on shallow water, whose solution yields a sinusoidal shape of bore wave surface. Good results can be obtained with the use of Korteweg de Vries equation, whose solution is a cnoidal wave function [20]. Measurement data and mathematical models are in good agreement, although neither the linear wave theory, nor the cnoidal wave function can describe the asymmetrical shape of the bore wave and the details of free water surface profile [20, 25].

Turbulent Flow Structure in an Estuary in the Presence of a Bore

Observations of tidal bores in nature show them to cause strong turbulent mixing in the estuarine zone with the effect extending over considerable distances [20]. In a river mouth area where a bore forms, a reverse current appears, the longitudinal velocities U_x rapidly decrease at all horizons, and pulsations of all three velocity components downstream of the bore increase. In a flume model of bore, the passage of the wave of breaking bore causes a nearly 30-fold increase in the turbulent stresses ($\mathrm{Fr}_b \geq 1.8$) as compared to the bore regime without collapse [20]. In that case, Reynolds stresses are 1–2 orders of magnitude greater than the threshold of stress that causes the motion of bottom and suspended sediments in river flow. Thus, the tidal bore is accompanied by strong turbulization of flow, causing intense water mixing in the channel flow, which cannot be described by classical mixing theories.

The formation of large turbulent vortexes downstream of bore front, which follow the bore in the upstream direction, was also revealed with the use of up-to-date methods of numerical modeling [27]. Those vortexes stay near the bed while the bore is moving upstream and they can transport sediments and saline water in this direction. The results of physical and numerical modeling show the existence of wide variations in the transverse and vertical velocity components, suggesting the alternating currents behind the bore front. Signs of turbulence focuses were observed for undular and breaking bores, and the rate of vorticity generation was proportional to $(\mathrm{Fr}_b - 1)^3$ [33]. Vorticity clouds behind the bore are due to the secondary currents; those clouds increase because of the nonprismatic shape of the channel and its complex bathymetry. The transfer of large turbulent formations behind bore front was observed in the estuary of the Daly R. (Northern Australia) in the form of vortexes rotating clockwise and counterclockwise ~20 min after the passage of the bore [49].

A fundamental difference was found to exist in the turbulent structure of flows at the passage of a undula ($\mathrm{Fr}_b < 1.8$) and a weakly breaking ($1.8 < \mathrm{Fr}_b < 2.1$) bore [38], consisting in the difference between the pressure

and velocity fields behind the bore front. When a undular bore passes, large values of Reynolds stress form in the bottom part of the flow immediately after the passage of wave crest before the next crest. In the case of a weak breaking bore, large values of turbulent stresses were recorded in the shift zone at high velocity gradients, while a reverse vortex current was recorded at the bed.

Turbulent Diffusion Coefficients

Turbulent diffusion coefficients in a flow at the passage of a tidal bore can be determined in Lagrangian representation with the help of flow visualization and the measurement of the mean square of particle displacements σ_x and σ_y in the longitudinal and vertical directions, respectively. Under the approximation of homogeneous turbulence [44], the coefficients of longitudinal (D_x) and vertical (D_y) diffusion are

$$D_x = \frac{\sigma_x^2}{2t'}, \quad D_y = \frac{\sigma_y^2}{2t'}, \tag{5}$$

where t' is time scale; in moment $t' = 0$, the particle passes before the leading section of bore front.

In [21], the paths of motion of light spherical particles with diameters 3.72 ± 0.2 mm and the relative density of 1.037 ± 0.012 were recorded in a flume model, simulating the propagation of a surge wave. The obtained dimensionless coefficients for the undular and breaking bores are $D_x/U_1 d_1 = 0.1$, $D_y/U_1 d_1 = 0.018$; $D_x/U_1 d_1 = 0.12$, $D_y/U_1 d_1 = 0.011$, respectively, at the flow velocity before the undular bore $U_1 = 0.335$ m/s and that before the breaking bore $U_1 = 0.515$ m/s. The coefficients of longitudinal diffusion are an order of magnitude greater than the coefficients of vertical diffusion, and the coefficient of vertical diffusion for a undular bore is larger than that for the breaking one because of the long-time effect of free-surface oscillations.

To compare the values of $D_y/U_1 d_1$ in a bore wave with the depth-averaged coefficient of vertical diffusion in river flow $\overline{K_y}$, we will use expressions from [44]:

$$\overline{K_y} = 0.067 u_* H$$

or from [2]:

$$\overline{K_y} = 0.066 \kappa n \langle u \rangle H, \tag{6}$$

where u_* is friction flow velocity; κ is Karman constant; n is the exponent in the power law of velocity distribution; $\langle u \rangle$, H are the vertically averaged velocity and the river flow depth, respectively. Within the range of variations of n values, typical of lowland rivers (n = 0.1–0.3), the values of the standardized coefficient of vertical diffusion vary within the range $\overline{K_y}/\langle u \rangle H$ 0.0026–0.008, which, on the average, is an order of magnitude less than that in the flow during bore wave passage. Such increase in the coefficients of turbulent diffusion at the passage of a bore in a flow contributes to complete mixing of flow in the section where bore wave forms.

PROPAGATION OF SEAWATER INTO RIVER MOUTHS AND THE FORMATION OF BORE

Assessment of the Type of Water Mixing and Stratification at River Mouths by W/P_t

The distance of seawater penetration and the laws of its mixing with river water at river mouths are determined, as well as the existence of bore, by the ratio between the tidal magnitude, river runoff, and the rate of changes in the width and depth of the estuary. The penetration of seawater into river mouths is typical of the estuaries of the rivers of Seine, Gironde, Mersey, Severn, and Mezen and the mouths of estuarine–deltaic type according to V.N. Mikhailov's classification [8] (Hooghly Branch of the Ganges R., the Northern Branch of the Yangtze R.). In the deltas of rivers with small bed slope toward the sea, seawater intrusion into their branches is weak.

The intrusion of saline water into a river mouth depends on the type of mixing of sea and river water, which is determined by the flow ratio of freshwater W to seawater P_t entering the estuary during flood tide [3, 6, 32, 46]. When $W/P_t > 1$, a "saltwater wedge" will form; at $0.1 < W/P_t < 1.0$ and $0.005 < W/P_t < 0.1$, the estuary shows partial mixing with strong and weak stratification; and at $W/P_t < 0.005$, the estuary is mixed completely. All mouth areas, for which estimating W/P_t is possible (Table 1), refer to partially mixed estuaries with weak stratification (Qiantang R., the Northern Branch of the Yangtze R., Hooghly Branch, the rivers of Mezen, Seine, and Gironde) and completely mixed (Severn, Mersey). The peculiarities of calculating W/P_t for different mouths and its changes due to channel-training operations are described below.

The Position of Bore Boundary and Seawater Penetration into the Mouths of Some Rivers

A detail description of the Amazon delta, the river's runoff, and the hydrological processes in it is given in [7]. The estimation of W/P_t for Amazon delta branches is difficult because of the scarcity of data on water flows in individual branches and their areas. Observations show that pororoka bore forms in estuarine widening of Amazon branches at a distance of 10–20 km upstream of the mouth section and propagates over large distances upstream the branches. The height of the bore can reach 4 m. Because of the high flow in the river, reaching 1.7×10^5 m^3/s, according to refined data [7], and the specific geological structure of the offshore zone [28], saline water does not penetrate into river delta. In that case, "saline wedge" forms in the bottom layer of the ocean at the marine

Fig. 2. Mouths of (1) the Yangtze R. with (2) the Northern and (3) Southern branches and (4) the Qiantang R.; arrows show the directions of flows in the Northern Branch of Yangtze delta.

shelf of the Amazon [45]. The shape of the vertical salinity distributions varies depending on river runoff, but in the driest season at minimal flow, the "saline wedge" does not reach the mouth section of the Northern Branch. The tidal variations of water level during dry period extend over ~900 km upstream the river [7]. Thus, the bore has no effect on the transport of saline water into delta branches but plays a significant role in the transport of sediments, and appears to be a major cause of the absence of river delta protrusion [34].

At the river mouths where $W/P_t = 0.005–0.1$, the volume of the tidal prism is large enough relative to river runoff, and the tidal current is so strong that the motion of the entire water mass becomes turbulent and the bottom and top layers exchange mass and salt in both directions. In a weakly stratified estuary, water salinity in the top and bottom layers gradually increases toward the sea. In the vertical salinity profiles, the salinity gradually increases from the surface to the bed with a maximal gradient near the interface between the layers.

The "Silver Dragon" bore with a wave up to ~4 m in height (largest in the world) forms at the mouth of the **Qiantang R.**, flowing into Hangzhou Bay, East China Sea. The mean tide range at the eastern coast of China (Fig. 2) is 3.3 m [29]. Near the mouths of the Yangtze and Qiantang rivers, the tide range increases because of the narrowing of the bays, reaching 9 m (the maximal value on China coast) in Hangzhou Bay and at Ganpu Town [41] (Fig. 3a). River runoff is small, except for high-flood periods; the normal annual water flow in the river at the Hangzhou section $Q =$ 1000 m^3/s (Table 1). The volume of the tidal prism is very large (~ 5.3×10^9 m^3) and comparable with the tidal prism of the Yangtze R. [23], and the ratio W/P_t is small (0.01 [31]), leading to periodic manifestations of weak stratification of estuarine water masses, which are commonly mixed over the vertical. Global channel training operations were carried out in this estuary in the 1960s–1990s with the aim to reduce the surface area flooded by tides. The hydrological regime of the estuary changed significantly because of this activity.

The estuary of the **Hooghly Branch** in the mouth area of the Ganges and Brahmaputra ranks next in terms of bore size. The hydrological regime of this area was described in detail in [10]. The estuary of the Hooghly Branch, ~80 km in length, extends from the mouth section at the level of the western extremity of Sagor Island (28 km in width) to Diamond Harbor Town (Fig. 4a). The monsoon climate of this domain determines the uneven distribution of water runoff in the Hooghly Branch during the year. Water flow (Q) in the branch in monsoon season (June–September) averages 1400–2300 m^3/s with maximum $Q =$ 2500–3500 m^3/s [5]. According to new data given in [40], the averages over 1998–2001 of the water flow entering the branch from the runoff-controlling dam Farakka (commissioned in 1976) are 1000 ± 81.6 in the dry period from February to May, 2975 ± 1144 during monsoons, and 1875 ± 985.5 m^3 from October to January. The mean annual Q in the branch after the construction of the dam is 1950 m^3/s. With the minimal Q used for the assessment of W/P_t, we have $W/P_t = 0.03$, and with the mean $Q = 1950$ m^3/s, $W/P_t = 0.06$, i.e., the flow in the estuary is vertically mixed with weak stratification.

The range of tide varies along the shelf from 5.6 in the east to 3.8 in the west [10], the range of the spring tide at the mouth of Hooghly branch reaches 4.9 m. The tidal water level variations propagate over 300 km upstream the branch. In the reach upstream Diamond Harbor Town, the depth decreases to 4 m, the height of the tidal wave gradually increases, and, between the towns of Hooghly Point and Brul (37 km downstream of Calcutta), the wave becomes much steeper, forming a tidal bore ~1.5 m in height over large depths and up to ~3.5 m on shallows [24]. Until the 1940s, the bore appeared during equinoctial spring floods, while since the 1960s, it has appeared during each spring flood tide. The main cause of the increase in bore frequency

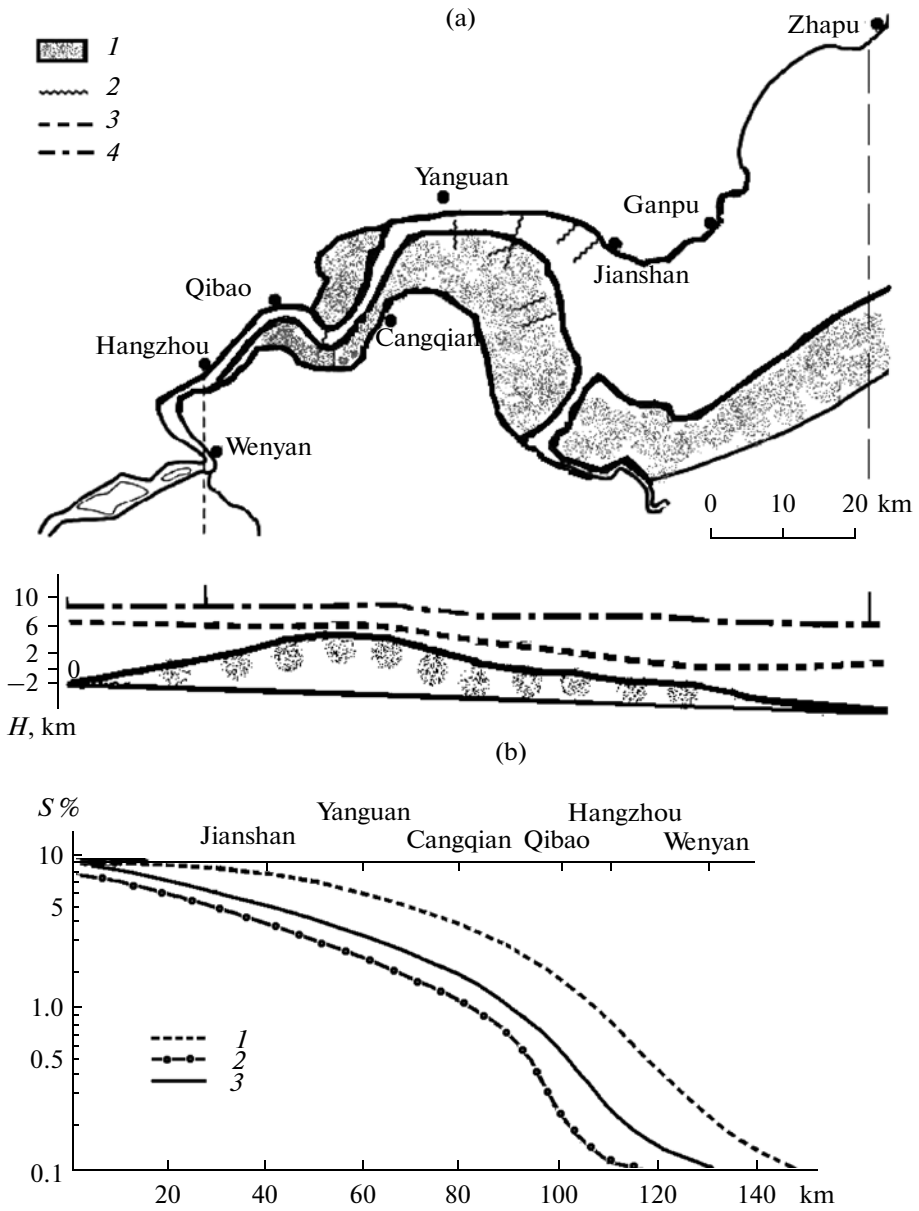

Fig. 3. (a) Scheme of the estuary of Qiantang R. before and after channel training operations : (*1*) drained areas, (*2*) the positions of sections in which bore waves form; the inset shows a sand bar and the mean (*3*) ebb and (*4*) flood water levels. (b) Variations in the distribution of mean water salinity along Qiantang R. estuary: (*1*) before channel training, (*2*) after the commissioning of the reservoir in the upper river reaches, (*3*) after channel training and the commissioning of the reservoir. The distance is measured from the sea gage of the estuary at Ganpu T.

is the gradual decrease in water flow from the Ganges. The silting of the upper reaches of the tidal branch had some effect on the increase in bore frequency [5]. The highest tides were recorded from February to May and from July to September. The velocity of flood tide currents in the reach from the mouth section (the southwestern extremity of Sagor Island) to the section of Diamond Harbor varies from 0.5 to 2.0 (with the average of 1.2) m/s, the velocity of ebb tide currents varies from 0.2 to 1.4 m/s [40].

An increase in water salinity in the estuary is recorded at the least water flows before monsoon, the maximal salinity values were recorded in May. A decrease in water salinity, caused by an increase in river water flow, was recorded in monsoon period with a minimum during flood in September (Fig. 4b) [40]. The vertical salinity gradients are relatively small and vary within the ranges of 0.3–2.1 during dry season, 1.2–3.1 during monsoon, and 0.5–2.2‰ from October to January. Thus, Hooghly Branch mouth is a well-mixed estuary with weak water stratification, as is con-

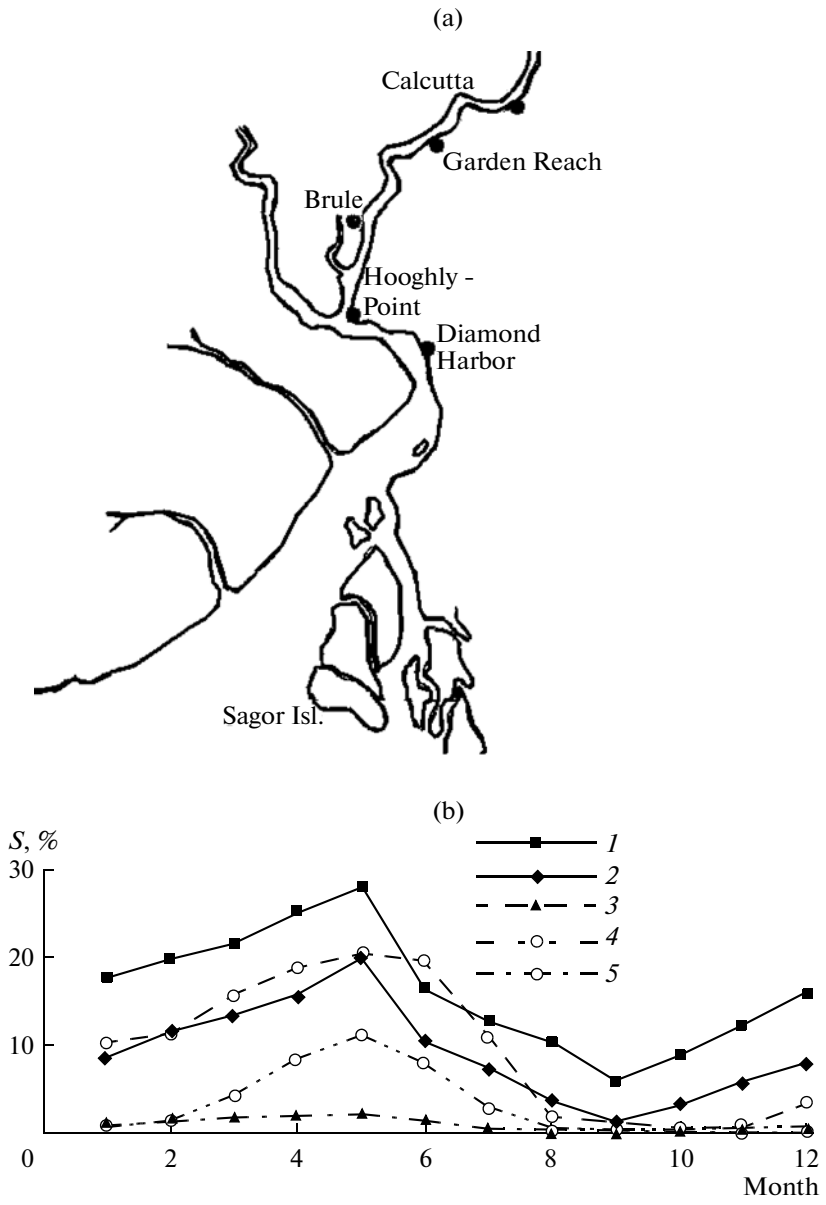

Fig. 4. (a) Plan of Hooghly Branch estuary and (b) the distribution of mean monthly water salinity in Hooghly Branch estuary over 1998–2001: (*1*) in the mouth section—the southwestern extremity of Sagor Isl., in sections—(*2*) the northern extremity of Sagor Isl. and (*3*) at Diamond Harbor after the construction of Farakka Dam [40], in sections (*4*) Diamond Harbor and (*5*) Garden Reach in 1958–1959 before dam construction [24].

firmed by the type of water stratification determined by parameter W/P_t.

Before the construction of Farakka Dam, saline water with $S \cong 10‰$ reached Garden Rich Town (Fig. 4b), and bore waves that form downstream from February to May contributed to the transfer of saline water up to Calcutta and further upstream. Nowadays, saline water never penetrates into Hooghly Branch mouth further than Diamond Harbor Town (Fig. 4b), which is ensured by runoff regulation at Farakka Dam [40]. The bore that forms upstream of Brul T. has no effect on the transfer of saline water upstream the branch, since it forms upstream of the boundary of saline water intrusion, similarly to the bore at the Amazon mouth.

The **Yangtze R.** delta in its head divides into the Northern and Southern branches, and, by its structure, it is similar to the Amazon delta [11] (Fig. 2). Near the sea, the Southern Branch bifurcates many times, while the Northern branch is a funnel-shaped estuary. Bore in the Northern Branch of the Yangtze R. has taken place since the 1940s. The frequency and the height of the bore in the Northern Branch are less than those in the Qiantang estuary. The narrowing of the

Northern Branch caused a considerable deformation of tidal waves and an increase in the height of bore in recent years. The general pattern of currents at the mouth is shown in Fig. 2 [26].

The Northern Branch is an estuary 80 km in length and mostly 2–4 m in depth (Fig. 5a). The width of the estuary at the mouth section is 16 km, and that at the confluence of the branches is ~3 km. The mean and maximal ranges of semidiurnal tides are 3.04 and 5.95 m, respectively. The evolution of the estuary is determined by its shape, hydrodynamic conditions, sediment transport, and, especially, variations in Yangtze water flow. The water flow steadily decreases since the early XX century, resulting in the transformation of the Northern Branch from a flow with dominating effect of ebb tide into one with dominating flood tide. The width of the Northern Branch continues decreasing with decreasing water flow. According to refined data, the normal annual water flow in the Yangtze is 2.82×10^4 m^3/s [11], the share of the Northern Branch being as little as 1.3% (367 m^3/s). Since the early XVIII century, when the major water flow turned into the Southern Branch, water flow in the Northern Branch dropped significantly and the branch became narrower, especially in its upper reaches (Fig. 5a). Some segments in the upper reaches became silty and shallow, while the mouth areas increased. Thus, the cross-section area at the mouth section at Lianxing-Port T. increased from 369000 m^2 in 1991 to 382000 m^2 in 1998 [22].

Tidal bores of three types form in the Northern Branch: (1) with low, not breaking crest, whose height varies from 10 to 30 cm; (2) linear bore with breaking crest more than 30 cm in height; (3) return bore, which forms at strong bore, which reaches the upper boundary of the Northern Branch and reflects from the flow in the Southern Branch. In Qinlong Port, return bore will take place 1–1.5 h after the passage of direct linear bore. The height of the return bore can be equal or greater than that of the direct bore [22].

The section in which bore forms during the propagation of tidal wave into the estuary and which is referred to as the bore boundary, is determined by the condition $\mathrm{Fr}_b > 1$. The bore boundary moves, depending on the tidal phase, either downstream at the maximally high tide or upstream at the relatively low tide. For the minimal (h_b = 0.3 m) and maximal (h_b = 1.6 m) bores, recorded in Qinlong Port in the shallow (~1.5 m) Lingdianxi section, $\mathrm{Fr}_b > 1$ (1.21 and 1.29, respectively [22] (Fig. 5a)). Further downstream in the branch, $\mathrm{Fr}_b < 1$; while upstream, up to Qinlong Port, $\mathrm{Fr}_b > 1$. Thus, the section at Lingdianxi can be taken as the boundary of formation of a bore, which transfers upstream water masses with homogeneous salinity from this area.

As the level rises during spring tide, seawater penetrates into the mouth through the Northern and Southern branches; in the Northern Branch, it reaches the western extremity of Chongming Island, where it meets the flow from the Southern Branch. The reverse flow in the Southern Branch stops at the level of the middle of Chongming Island because of the larger river water flow. During ebb tide, the seawater that penetrates into the Southern Branch through the Northern Branch mixes with the water of the Southern Branch and moves toward the sea.

Water salinity in the Northern Branch varies within 5–14‰, i.e., it is much higher than that in the Southern Branch (0–3‰). During dry season, the net water flow is negative, i.e., directed toward the river, and saline water reaches the mouth mostly via the Northern Branch. Figure 5b shows the distributions of the section-averaged water salinity along the Northern Branch at spring and neap tides. Water salinity in the same sections during syzygy is less than during neap. Upstream of section 3, water salinity steadily decreases at any tide heights, thus suggesting the good water mixing and dilution in this area. Due to the implementation of the project of Northern Branch narrowing and the construction of a sluice [26], water salinity in the branch, where it meets the Southern Branch water, is nearly zero whatever the tide range. Thus, during rising tide, saline water does not penetrate into the Southern Branch, while during water fall, the 0.25‰ isohaline (the standard 0.25‰ is accepted in China) moves from the Southern Branch into the open sea; this fact is of importance as the water intake of Shanghai City is situated here.

Gironde Estuary is a part of the mouth area of the Garonne and Dordogne rivers [12]; therefore, the Table 1 gives the total value of Q for those rivers. The volume of the tidal prism, calculated by the tide rate and used to evaluate W/P_t (Table 1) is in agreement with the value $P_t = 2 \times 10^9$ m^3 obtained in [12]. Measurements show that a residual seaward current exists in the surface water layer, and a landward one, in the bottom layer, as is confirmed by the type of estuarine circulation determined by parameter W/P_t, given in Table 1.

According to data in [12], the upper boundary of the estuary, i.e., the penetration boundary of saline water into the estuary, lies near the confluence of the rivers of Garonne and Dordogne. A bore with a high, rapidly collapsing crest forms in a shallow reach in the Garonne R. upstream of Bordeaux; while in the Dordogne R, at Saint-Pardon Town (30 km upstream of the Gironde estuary head), a wavy bore forms with a wave chain propagating 30 km upstream [35]. Thus, the bore forms in the mouth areas of the Garonne and Dordogne rivers a long distance upstream of the upper boundary of the estuary and the boundary of seawater penetration into the estuary, so it has no effect on seawater transport, but contributes much to sediment transport along those reaches.

In the fully mixed estuary at $W/P_t < 0.005$, turbulent mixing becomes strong enough to eliminate the local salinity variations. The salinity grows with approaching the sea but remains constant over depth;

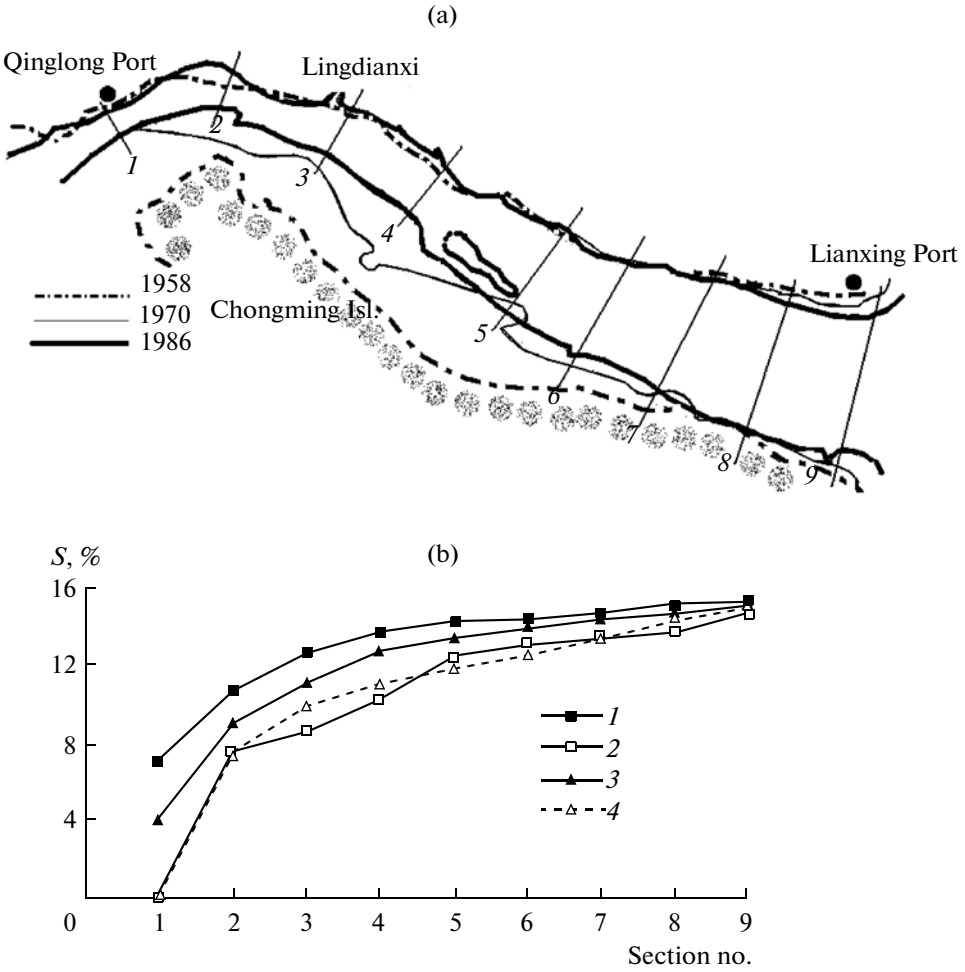

Fig. 5. (a) Evolution of the bansk of the Northern Branch of the Yangtze R. and the positions of gages in which water velocity and salinity were measured and (b) the distribution of section-averaged water salinity along the Northern Branch during maximal and minimal (*1, 2*) spring and (*3*, *4*) and neap tides.

no top or bottom layers can be identified. The very weak, as compared with the strong tidal current, mean current is directed seaward at all depths, and the penetration of salt into the estuary takes place exclusively due to turbulent diffusion in the averaged current.

Mersey R. estuary, according to [18], is 46 m in length, extending from the mouth section in New Brighton T. to the tide propagation boundary in Warrington T. A reach, referred to as Narrows (1–1.8 km in width, ~20 m in depth) begins upstream of New Brighton and extends 10 km upstream past Liverpool to Dingle area (Fig. 6a). The area as a whole is referred to as the lower estuary, while that from Dingle to Warrington T., as the upper estuary. The main water flow passes through the Manchester navigation channel [18] and empties into the upper estuary near Eastham T.

During the measurements of the velocity and salinity in June–July, the mean water flow at a site 2 km upstream of New Brighton (the lower estuary) was 80 m^3/s [18]. The depth-averaged velocity of tidal current is 0.9 m/s during neap tide and 1.3 m/s during spring tide. The structure of currents in the estuary is different during flood and ebb tides. Water salinity measurements in the lower estuary showed the salinity to be uniform over depth during neap tide, whereas during spring tide, the difference between water salinity in the surface and bottom layers never dropped below 0.5‰. The absolute values of salinity vary from 25‰ on the surface to 31‰ at the bed. The flow in the lower estuary is transitional from the strongly stratified to moderately stratified [18]. The reverse density flow in the lower estuary was found to increase with increasing tide amplitude at constant river flow. The authors of [42] also assume the current in the estuary partially mixed. On the other hand, in [39], with the flow considered in the entire estuary, the vertical salinity gradient was zero, and the flow was completely mixed during ebb tide due to the abrupt narrowing of the flow near Liverpool and the large flow velocities. The ratio $W/P_t \sim 0.001$, calculated by the mean estuary characteristics, also shows that water mixing is

complete. It is likely that the flow structures in the lower and upper estuaries of the Mersey R. are different and it should be divided, notwithstanding its small size, into the lower and upper estuaries, like the estuary of the St. Lawrence R. [3].

The range of the neap tide at the entry to the estuary is 4 m, and that of spring tide may reach 10 m. The bore forms in the estuary at the tide range of ~10 m, which has been recorded in periods near the spring and autumn equinoxes. However, the bore can form at a lower tide, when the river flow decreases during dry season. Bore forms in the upper estuary of the Mersey R. at Hail dam (~30 km from the mouth area) about 2 h 25 min before high water in Liverpool. From the park on the right-hand bank, one can see its passing under the railway and motorcar bridges of Runcorn T. ~1 h 50 min before high water in Liverpool. Under favorable conditions, the bore reaches Warrington, passing under the railway bridge 20 min before high water in Liverpool, rapidly passes by the downtown, and reaches the dam upstream of the city immediately before high water in Liverpool. Water salinity at the depth of 0.6 m from the surface (Fig. 6b) in the site of bore formation at Hail dam is 12‰ [18], i.e., the bore facilitates the upstream transfer of water with a salinity that can persist for a long time, if the river flow is small.

The coefficients of turbulent diffusion, calculated by the results of measurements in the Narrows of the lower estuary of the Mersey R. are as follows: the longitudinal $D_x = 1.2–4.7 \times 10^2$ m^2/s [19] and the vertical $D_y = 12–37$ cm^2/s [18].

Severn R. estuary has a classical funnel-like shape; by the type of river and sea water mixing, it is similar to the Mersey estuary, so they are often compared in the scientific literature [43]. In Bristol Bay and in the mouth section at Minehead Cape in Severn Estuary (Fig. 7), the tide range reaches 15 m (ranking second after the largest one in Fundy Gulf (USA), reaching 18 m). In the literature, Gloucester City is considered as the head of the estuary [47]. The funnel-like shape of the estuary, the high tides, and the underlying surface, composed of hard rocks, pebble, and sand, facilitate the formation of flow with high turbidity, which embrowns the estuarine water. Water level variations during high neap tide reach the dam in Gloucester. During neap tides at Sharpness-Docks, a bore with the mean height of 1.5 forms; the maximal wave height (2.8 m) was recorded on October 15, 1966. The wave moves upstream the river with a high velocity of 5–8 m/s, and it can be seen as far as 4 km downstream of Gloucester.

The authors of studies devoted to measurements of water salinity in the Severn estuary mention the absence of vertical salinity gradient in estuarine water [16, 43, 47], which is also confirmed by the value of parameter $W/P_t = 0.001$. The upper boundary of the propagation of saline water during spring tide lies between Epney and Gloucester, while in the neap tide, it never rises upstream Arlingham [16]. In winter, river floods shift the boundary of saline water seaward. Water salinity in the estuary shows wide tidal and seasonal variations, though it is more or less stable in some areas. In summer, the zone of stable salinity reaches Aust T., and the zone of wide salinity variations is situated upstream of Sharpness-Docks. The maximal rate of salinity variations in Apny in the period of summer neap tides reaches 15‰ [17]. The widest salinity variations, caused, in particular, by saline water transport by bore waves, penetrate into Arlingham, where during a tidal cycle in summer, they can reach the maximal value of 15‰ at the maximal rate of changes of 15‰/h; during a week, water salinity can change from 0 to 25‰. The most stable conditions in terms of water salinity were observed in Aust in summer, while in the section at Arlingham, the most stable are low salinities at high water in winter. In Aust, water salinity in summer is nearly constant—~25‰ with variations within 2‰ depending on tidal phase. In winter, the mean water salinity in spring tide is ~14‰ with variations within 2‰ depending on tidal phase. At neap tide, salinity variations during tidal cycle reach 10‰ and the mean salinity can drop to zero. In winter, the zone of stable salinity extends upstream to Weston, and the zone of strong variations of water salinity shifts to Aust. The minimal rate of salinity variations was recorded in Aust during winter neap tides, when it never exceeds 2‰/h. The bore that forms in the section at Sharpness-Docks plays a significant role in the formation of the zone of abrupt salinity variations at Arlingham.

The coefficient of longitudinal dispersion in Severn estuary increases upstream from ~10^2 m^2/s at the mouth section to ~10^3 m^2/s in estuary head [48]. The coefficient of vertical turbulent diffusion, measured near mouth section and averaged over several tidal cycles is ~100 cm^2/s [47]. For example, D_y, in Severn estuary is several times greater than that in Mersey estuary, i.e., the vertical mixing in Severn estuary is more intense, notwithstanding the same values of W/P_t parameter, estimated by the mean characteristics of the estuaries.

THE EFFECT OF CHANNEL-TRAINING OPERATIONS ON SEAWATER INTRUSION AND THE FORMATION OF BORE AT SOME MOUTHS

Qiantang R.

At its inflow into Hangzhou Bay, the Qiantang R. forms a wide and shallow estuary. The bay width along the delta coastline is 100 km; it has a funnel-like shape, becoming narrower toward river mouth; the width of the sea section of the estuary at Ganpu T. is 20 km. As mentioned above, the height of tides at Ganpu reaches the maximal value for the coast (9 m) [41]. The flow width B at estuary head near Hangzhou T. is ~1.2 km [31]. The depth H varies from 1–6 m during ebb tide to 10 m at high water. The width

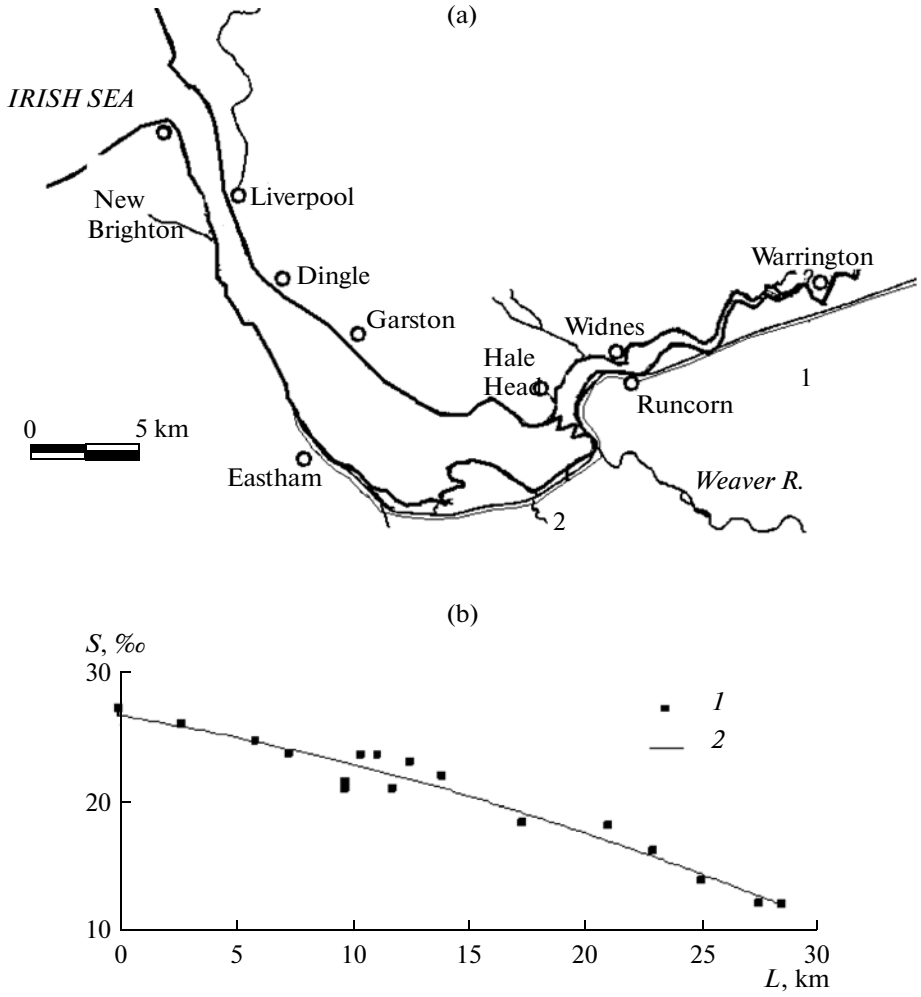

Fig. 6. (a) Schematic map of Mersey R. estuary: (a) (1) Manchester navigation channel, (2) the position of bore formation section; (b) water salinity distribution in the midstream along the estuary [18]: (*1*) measurements, (*2*) data extrapolation.

to depth ratio $\sqrt{B}/H > 10–45$, which is greater than such ratio for the Yellow R., a typical divagative river in China.

The length of the mouth area of the Qiantang R. from the sea section of the estuary to the boundary of tide penetration into the estuary is 282 km [31]. The entire mouth area of the Qiantang R. is divided into 3 zones (Fig. 4a): the upper zone, which is subject to the effect of the river and extends over 78 km upstream Wenyan T., where the penetration boundary of tidal level variations lies; the middle zone, i.e., the estuary proper, extending from Wenyan T. to Ganpu T.; its length is 122 km; the lower zone (nearshore area), which is subject to the effect of tides, is the part of Hangzhou Bay between the towns of Ganpu and Lucaogan 82 km in length. The upper and lower reaches are relatively stable, whereas in river estuary, enormous tidal currents with a high tidal bore form in several sections upstream Jianshan T. (Fig. 4a). Bottom sediments in this reach are well-sorted, homogeneous, readily scoured silts with particle diameters of 0.02–0.04 mm, which facilitate strong aggradation and erosion of the channel. The main channel permanently changes its position and, accordingly, the area of lowlands flooded by tidal waters changes permanently. From the north and the south, the estuary is surrounded by fertile valleys, whose surface lies 2–4 m below flood tide level; they are protected from tidal waves by levees.

The mean $Q = 1000$ m^3/s (Table 1) is small relative to the tidal prism volume. The result is that the large amount of sediment delivered by tidal current, cannot be carried away by weaker but longer lasting ebb current. The process of sediment accumulation causes the formation of a long inner bar (Fig. 4a), which causes the formation of a very wide and shallow channel, a strong tidal bore, frequent changes in the position of the main channel, and unstable foreshores.

To stabilize the shifting channel; to develop lowlands, flooded by tides, and to improve the navigation conditions, channel-training operations were carried

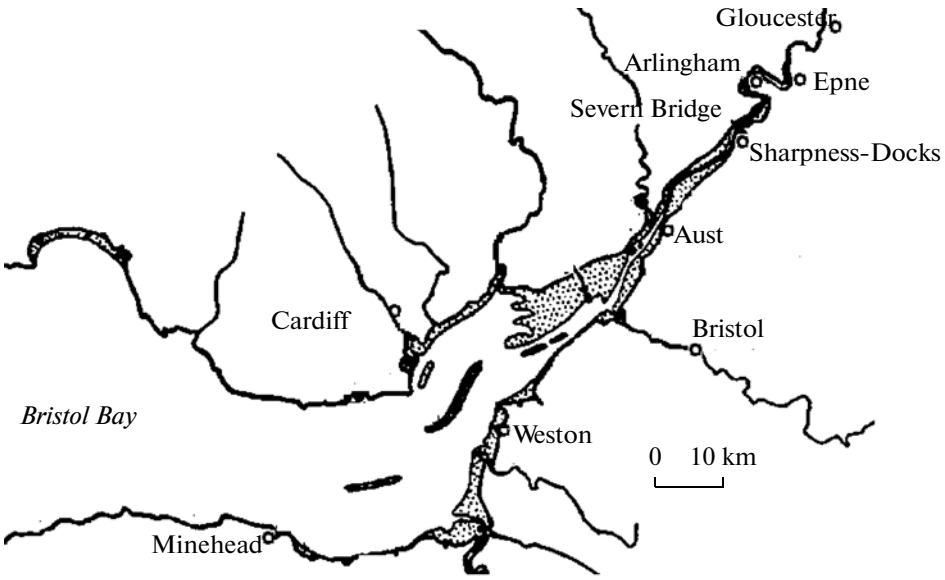

Fig. 7. Plan of Severn R. Estuary.

out in the past 50 years with the major aim to increase the W/P_t ratio by decreasing the volume of the tidal prism in the river segment from Hangzhou to Ganpu [31]. One-dimensional and two-dimensional numerical models, describing the motion of flow in the estuary, salt and sediment transport, and bore wave propagation were used to assess the efficiency of the proposed works [31]. The result of channel improvement in Qiantang R. estuary, the channel width in different sections was reduced 2–4 times (Table 2, Fig. 4a), and the total area available for industry and agriculture increased by 730 km^2. The main channel, 74 km in length was stabilized, and the relatively short hazardous segments within a reach of 200 km of leveed banks were reinforced.

The channel training operations were not aimed to eliminate bore; moreover, considering that the highest in the world bore forms at the mouth of the Qiantang R. and many tourist visit the site to see it, the aim was to preserve the bore. After channel training, the tidal level in a direct segment of the river increased by 27–41 cm. The increment of the ebb level in the middle reach is greater than those in the lower and upper gages [31]. Therefore the tide amplitude decreases in the middle and increases in the upper and lower reaches. In the curved segment of the river, both flood and ebb level drop, the ebb tide levels decreasing more significant that the flood ones, hence an increase in the tide amplitude. The general tendency is a rise of the flood tide level (Table 2) and its gradual increase upstream the river in a rectilinear river reach. The ebb levels upstream of Jianshan vary due to sediment erosion/deposition in the channel, and the tide amplitude varies accordingly. Riverbed deformations have no effect on the ebb tide levels at Ganpu and Zhapu gages, while flood tide levels increase due to the narrowing of the flow upstream the river; therefore, the amplitudes of tides increase.

During syzygy, the dynamic impact on levees and the intrusion of salt water is much stronger than during medium tides. After channel training, the flood–ebb levels and tide amplitudes increased in 90% of cases for syzygy and in 50% of cases at medium tides. After channel training, the increase in the flood/ebb water level in syzygy causes larger tidal flow velocity and stronger reflection of the tidal wave. Table 3 gives the cases where tidal water levels exceeded various water level rises within the year in the rectilinear river reach before and after channel training (1955, 1995). After channel training, water level during the appropriate tidal phases increased 1.16–13.1 times relative to that before training. The maximal water level increase was recorded in Qibao; it decreased at stations further downstream.

The length L of saline water intrusion into Qiantang R. mouth changed as the result of channel training [30] and river runoff regulation. Under natural regime, L is ~150 km; under runoff regulation, it is ~120 km; and after channel training, it is ~130 km (Fig. 3b). The total effect of runoff regulation and channel training was a decrease in L by ~20 km.

Seine R.

In the XIX century, one of the highest and the most hazardous bores took place in Seine estuary. The crest height reached 7.5 m, and the propagation velocity was up to 10 m/s [12]. The bore propagate over a distance of 80 km from the estuary mouth section at Trouville and reached Rouen, creating hazard for nav-

Table 2. Variations in the characteristics of Qiantang R. estuary due to the drying of part of the area of foreshore and channel training [31] (A is the cross-section area, B is the width, H is the mean flow depth, h is the tide height in the section under consideration, Q_e and q_e are water flow and specific water flow during ebb tide; here and in Table 3, the top and bottom values of the characteristic were obtained before and after channel training)

Gage	B, m	H, m	A, m^2	h, m	$P_t \times 10^8$, m^3	Q_e, m^3/s	q_e, m^2/s
Cangqian	2059 1802	1.8 174	3688 3130	1.75 2.01	0.80 0.70	3625 3333	1.76 1.84
Yanguan	4097 1806	2.87 3.0	11870 5440	4.15 3.73	3.0 1.85	10386 6915	2.53 3.82
Jianshan	16740 8415	3.1 3.75	52180 28250	4.58 4.42	10.0 5.0	33000 17270	1.97 2.05

igation in this reach. The activity of bore waves facilitated the formation of migrating mouth bars. Lower bore waves were also seen in Seine tributaries [36].

The parameter W/P_t, calculated for the estuary area $F = 104.5$ km^2, obtained from up-to-date space photographs [4], is 0.024. After channel training and the construction of levees in Seine channel from 1834 to 1978, the estuary area decreased by ~4 times (from 129.5 to 31.0 km^2) [13]. Calculations with those data yield $W/P_t = 0.08$, i.e., the role of river runoff have decreased during 33 years. After the start of channel training, the bore disappeared, and some time later, it appeared again, because of the gradual decrease in the depth due to channel filling with sediments. Regular dredging operations aimed to ensure stable navigation depth have led to an increase in the depth from 3 m under natural conditions to 6 m. After that, the bore disappeared completely.

The penetration distance of saline water into Seine estuary is steadily decreasing because of the elongation of artificial sand dams at estuary mouth and a decrease in the area of the estuary because of its silting [13]. The small depth and the artificial decrease in estuary width lead to complete mixing of river and sea waters in the estuary and the absence of two-layer circulation, typical of deeper estuaries. In 1955–1956, in low-flow period, saline water penetrated over a distance of 70 km from the mouth section. By now, the boundary of maximal penetration of saline water have shifted 20 km downstream because of channel training and the elongation of dams.

DISCUSSION OF RESULTS

The most important conditions for bore formation are tide range and the shape of the estuary. The analysis of the geographic position of some river mouths, where bore waves form, suggests that there is no clear threshold of maximal tide required for a bore wave to form. For example, in the Northern Branch of the Yangtze R., the bore forms at a relatively low tide with $h = 3.3$ m, while in Amazon branches, it forms at $h = 6.0$ m.

The shape of the estuary is characterized by the rate of flow narrowing dB/dL and the rate of depth change dH/dL (L is the distance along the river). The parameter dH/dL appears significant for bore formation. To confirm this idea, let us consider the Mezen River, whose estuary has a classical funnel-like shape. In the mouth section of this estuary (Maslanyi Cape–Ryabinov Cape [1]), the range of spring tide reaches 7.8 m, i.e., the tide height is sufficient for a bore to form. The length of the estuary from the mouth section between the capes of Maslyanyi and Ryabinov to Mezen T. is ~40 km. By parameter $W/P_t = 0.03$, Mezen estuary refers to the type of partially mixed estuaries with weak stratification. The rate of width change $dB/dL \cong 0.2$ is typical of the mouth of estuarine type. The depth in the mouth section of the Mezen R. is ~5 m; the flow velocity during tide cycle varies from −1.4 to 1.4 m/s [1]. In summer, the normal annual water salinity in the mouth section is nearly the same on the surface and in the bottom layer (28‰), while further upstream, it drops to 14‰ in Okulovo V. (16 km from the mouth section). In other seasons of the year, water salinity in the bottom layer is somewhat greater (2–4‰) than at the surface. This means that the estimate W/P_t adequately describes the type of water mixing and stratification in the estuary. The height of the tidal wave increases for some time during wave propagation into the estuary [1], but not enough to form a bore wave. The depth of Mezen estuary gradually decreases with a mean slope of $dH/dL \cong 1.3 \times 10^{-2}$, thus hampering the formation of a bore. The Froude number calculated for this estuary by the flow velocity and the depth in the mouth section $\mathrm{Fr}_b = 0.5$, i.e., it is half the threshold value of the bore $\mathrm{Fr}_b = 1$.

CONCLUSIONS

The description of a bore with the help of equations for a quasistationary hydraulic jump makes it possible to determine the critical Froude number for a flow, at which a tidal wave becomes a bore: $\mathrm{Fr}_b \geq 1$.

The main conditions for a bore to exist in an estuary are the tidal range not less than 3–4 m and the rap-

Table 3. Variations in the number of cases when water level rose above the specified value Δh per year at different stations along Qiantang R. estuary in 1955 (before straigtening) and 1995 (after training)

Station	Δh, m	N_1 (1955)	N_2 (1995)	N_2/N_1
Zhapu	>5.5 5–5.5	18 89	44 137	2.4 1.54
Ganpu	>6.5 6.0–6.5	2 31	6 61	3 2
Yanguan	>6 5.6–6.5	30 121	181 141	6 1.16
Cangqian	>7.0 6.5–7.0	65 102	163 120	2.5 1.18
Qibao	>7.5 7–7.5	7 27	92 127	13.1 4.7
Hangzhou	>8 7.5–8.0	7 8	26 65	3.7 8.1

idly narrowing estuary shape. Analysis of the estuary narrowing parameter for seven river mouths, especially, for the Qiantang R. has shown that $dB/dL \geq 0.1$ is enough for a bore to exist.

The coefficients of turbulent diffusion of flow during bore wave passage are an order of magnitude greater than the coefficients of river flow; the former coefficients ensure complete mixing of water mass at the bore formation boundary.

The effect of bore wave on the upstream transfer of saline water depends on the position of bore formation in the channel. In some cases, where bore forms upstream of the boundary of saline water intrusion (the Amazon, Dordogne, Garonne rivers and the Hooghly Branch), it has no effect on the propagation of saline water. In the case of bore formation in the section, which is reached by saline water, the bore facilitates their complete mixing and upstream transport. The effect of bore on salinity variations is most pronounced in Severn estuary.

Considerable artificial reduction of estuary area causes an increase in the distance over which saline water penetrates into the mouth. To reduce this distance during the draining of part of estuary area, it is necessary to take additional measures for river runoff regulation. The deepening of the navigation channel causes the elimination of bore.

ACKNOWLEDGMENTS

This study was supported by the Russian Foundation for Basic Research, project no. 10-05-00061.

REFERENCES

1. Demidenko, N.A., Efimova, L.E., Efremova, N.A., and Yurkin, M.M., Hydrometeorological Regime of Estuaries of the Mezen and Kuloi Rivers and its Possible Changes at the Construction of Mezen TPS, in *Ekologiya arkticheskikh i priarkticheskikh territorii, Mater. Mezhdunar. Simpoz.* (Ecology of Arctic and Near-Arctic Territories. Mater. Intern. Symp.), Arkhangel'sk, 2010, pp. 70–72.
2. Dolgopolova, E.N., Vertical Transfer Coefficient in Natural Streams, *Water Resour.*, 2008, vol. 35, no. 4, pp. 408–416.
3. Dolgopolova, E.N., and Isupova, M.V., Water and Sediment Dynamics at Saint Lawrence River Mouth, *Water Resour.*, 2011, vol. 38, no. 4, pp. 453–470.
4. Kravtsova, V.I., and Mit'kinykh, N.S., Mouths of World Rivers in the Atlas of Space Images, *Water Resour.*, 2011, vol. 38, no. 1, pp. 1–17.
5. MacDowell, D.M., and Connor, B.A., Gidravlika prilivnykh ust'ev rek (Hydraulics of Tidal River Mouths), Moscow: Energoatomizdat, 1983.
6. Mikhailov, V.N., *Gidrologicheskie protsessy v ust'yakh rek* (Hydrological Processes at River Mouths), Moscow: GEOS, 1997.
7. Mikhailov, V.N., Water and Sediment Runoff at the Amazon River Mouth, *Water Resour.*, 2010, vol. 37, no. 2, pp. 145–159.
8. Mikhailov, V.N. and Gorin, S.L., New Definitions, Regionalization, and Typification of River Mouth Areas and Estuaries as Their Parts, *Water Resour.*, 2012, vol. 39, no. 3, pp. 247–260.
9. Mikhailov, V.N., Gorin, S.L., and Mikhailova, M.V., A New Approach to the Determination and Typiphication of Estuaries, *Vestn. Mosk. Univ., Ser. 5, Geogr.*, 2009, no. 5, pp. 3–11.
10. Mikhailov, V.N., and Dotsenko, M.A., Peculiarities of the Hydrological Regime of the Ganges and Brahmaputra River Mouth Area, *Water Resour.*, 2006, vol. 33, no. 4, pp. 353–373.
11. Mikhailov, V.N., Korotaev, V.N., Mikhailova, M.V., et al., Hydrological Regime and Morphodynamics of the Yangtze River Mouth Area, *Water Resour.*, 2001, vol. 28, no. 4, pp. 351–363.
12. Mikhailova, M.V., and Isupova, M.V., Water Circulation, Sediment Dynamics, Erosional and Accumulative Processes in the Gironde Estuary (France), *Water Resour.*, 2006, vol. 33, no. 1, pp. 10–23.
13. Mikhailova, M.V., and Isupova, M.V., Water and Sediment Dynamics in the Estuary and Mouth Area of the Seine River, *Water Resour.*, 2007, vol. 34, no. 1, pp. 35–48.
14. Spitsyn, I.P., and Sokolova, V.A., *Obshchaya i rechnaya gidravlika* (General and River Hydraulics), Leningrad: Gidrometeoizdat, 1990.
15. Shterenlikht, D.V., *Gidravlika* (Hydraulics), Moscow: Energoatomizdat, 1991, vol. 1.
16. Bassindale, R., Studies on the Biology of the Bristol Channel: XI. The Physical Environment and Intertidal Fauna of the Southern Shores of the Bristol Channel and Severn Estuary, *J. Ecology*, 1943, V. 31, no. 1, pp. 1–29.

17. Bassindale, R., A Comparison of the Varying Salinity Conditions of the Tees and Severn Estuaries, *J. Animal Ecology*, 1943, vol. 12, no. 1, pp. 1–18.

18. Bowden, K.F., and Gilligan, R.M., Characteristic Features of Estuarine Circulation as Represented in the Mersey Estuary, *Limnol. Oceanogr.*, 1971, vol. 16, no. 3, pp. 490–502.

19. Bowden, K.F., and Sharaf, El Din, Circulation and Mixing in the Mersey Estuary, *Geophysical J. Royal Astronomical Society*, 1966, vol. 10, no. 4, pp. 383–399.

20. Chanson, H., Environmental, Ecological and Cultural Impacts of Tidal Bores Benaks, Bonos and Burros, *Proc. IWEH. Intern. Workshop on Environ. Hydraulics: Theoretical, Experimental and Computational Solutions. Valencia*, 2009, pp. 1–20.

21. Chanson, H., and Tan, K.-K., Turbulent Mixing of Particles under Tidal Bores: An Experimental Analysis, *J. Hydr. Res.*, 2010, vol. 48, no. 5, pp. 641–649.

22. Chen, S., Tidal Bore in the North Branch of the Changjiang Estuary, *Proc. Intern. Conf. Estuaries and Coasts. Hangzhou (China)*, 2003, pp. 1–8.

23. Chen, J., Li, D., Yao, Y., Li, J., and Jin, W., Marine Hazards in Coastal Areas and Human Action against Them - a Case Study of the Changjiang River Estuaries and Qiantang River, *Chinese J. Oceanology and Limnology*, 1999, vol. 17, no. 2, pp. 143–154.

24. Chugh, R.S., Tides in Hooghly River, *Hydrol. Sci. J.*, 2009, vol. 6, no. 2, pp. 10–26.

25. Donnelly, C. and Chanson, H., Environmental Impact of Undular Tidal Bores in Tropical Rivers, *J. Environ. Fluid Mechanics*, 2005, vol. 5, no. 5, pp. 481–494.

26. Fu, G., Chen, J., and Jiang, W., Scenario Studies on the Salinity Intrusion in the Yangtze Estuary. http://www.paper.edu.cn

27. Furuyama, S., and Chanson, H., *A Numerical Study of Open Channel Flow Hydrodynamics and Turbulence of the Tidal Bore and Dam-Break Flows*, Hydraulic Model Report no. *CH66/08,* Brisbane: University of Queensland, 2008.

28. Geyer, W.R., Beardsley, R.C., Candela, J., et al., The Physical Oceanography of the Amazon Outflow, *Oceanography*, 1991, April, pp. 8–14.

29. Guohong, F., Tide and Tidal Current Charts for the Marginal Seas Adjacent To China, *J. Oceanology and Limnology*, 1986, vol. 4, no. 1, pp. 1–16.

30. Han, Z., Pan, C., Yu, J., and Chen, H., Effect of Large-Scale Reservoir and River Regulation/Reclamation on Saltwater Intrusion in Qiantang Estuary, *Science in China (Series B)*, 2001, vol. 44, Supp. no. 8, pp. 221–229.

31. Han, Z., Xu, Y., Lin, B., and Xuan, W., Variation of Tides and River Regime after River Training in the Qiantang Estuary, *Intern. Conf. Estuaries and Coasts, Hangzhou*, 2003, pp. 66–80.

32. Hansen, D.V., and Rattry, M., Gravitational Circulation in Straits and Estuaries, *J. Mar. Res.*, 1965, vol. 23, pp. 104–122.

33. Hornung, H.G., Willert, C., and Turner, S., The Flow Field Downstream of a Hydraulic Jump, *J. Fluid Mech.*, 1995, vol. 287, pp. 299–316.

34. http://en.wikipedia.org/wiki/Amazon_River

35. www.tidalbore.info/france/gironde.html

36. www.tidalbore.info/france/seine.html

37. http://en.wikipedia.org/wiki/Tidal_bore# Rivers_with_tidal_bores

38. Koch, C., and Chanson, H., Turbulence Measurements in Positive Surges and Bores, *J. Hydr. Res.*, 2009, vol. 47, no. 1, pp. 29–40.

39. Mills, A.D., *A Dictionary of English Place-Names*, Oxford: Oxford University Press, 1998.

40. Mukhopadhyay, S.K., The Hooghly Estuarine System, NE Coast of Bay of Bengal, India, *Proc. Workshop on Indian Estuaries*, Goa: NIO, 2007, pp. 1–26.

41. Pan, C.-H., Lin, B.-Y., and Mao, X.-Z., Case Study: Numerical Modeling of the Tidal Bore on the Qiantang River, China, *J. Hydraulic Engineering, ASCE*, 2007, vol. 133, no. 2, pp. 130–138.

42. Pethick, J., *Review and Formalization of Geomorphological Concepts and Approaches for Estuaries. Technical Report FD2116/TR2*, London: Nobel House, 2006.

43. Prandle, D., Salinity Intrusion in Estuaries, *J. Physical Oceanography,* 1981, vol. 11, no. 10, pp. 1311–1324.

44. Roberts, P.J.R., and Webster, D., Turbulent Diffusion, *Environ. Fluid Mechanics—Theories and Application*,. Reston: ASCE Press, 2002.

45. Rosário, R.P., Bezerra, M.O., and Vinzón, S.B., Dynamics of the Saline Front in the Northern Channel of the Amazon River—Influence of Fluvial Flow and Tidal Range (Brazil), *J. Coastal Research*, 2009, vol. 56, Special Issue, pp. 1414–1418.

46. Tomczak, M., and Godfrey, J.S., *Regional Oceanography: an Introduction*, 2nd improved addition, Delhi: Daya Publishing House, 2003.

47. Uncles, R.J., and Jordan, M.B., Residual Fluxes of Water and Salt at Two Stations in the Severn Estuary, *Estuarine and Coastal Marine Science*, 1979, vol. 9, no. 3, pp. 287–302.

48. Uncles, R.J., and Radford, P.J., Seasonal and Spring-Neap Tidal Dependence on Axial Dispersion Coefficients in the Severn—A Wide, Vertically Mixed Estuary, *J. Fluid Mech.*, 1980, vol. 1, pp. 703–726.

49. Wolanski, E., Williams, D., Spagnol, S., and Chanson, H., Undular Tidal Bore Dynamics in the Daly Estuary, Northern Australia, *Estuarine, Coastal and Shelf Science,* 2004, vol. 60, no. 4, pp. 629–636.